DEVELOPING AND FIELD IMPLEMENTING A DYNAMIC ECO-ROUTING SYSTEM

Final Report

Hesham Rakha, Ahmed Elbery, Jinghui Wang

April 2017

DISCLAIMER

The contents of this report reflect the views of the authors,
who are responsible for the facts and the accuracy of the
information presented herein. This document is disseminated
under the sponsorship of the Department of Transportation,
University Transportation Centers Program, in the interest of
information exchange. The U.S. Government assumes no
liability for the contents or use thereof.

1. Report No.	2. Government Accession No.	3. Recipient's Catalog No.		
4. Title and Subtitle Developing and Field Implementing a Dynamic Eco-Routing System		5. Report Date April 2017		
		6. Performing Organization Code KLK900-SB-001		
7. Author(s) Rakha, Hesham; Elbery, Ahmed; and Wang, Jinghui		8. Performing Organization Report No. N17-003		
9. Performing Organization Name and Address National Institute for Advanced Transportation Technology University of Idaho 875 Perimeter Dr, MS 0901 Moscow, ID 83844-0901		10. Work Unit No. (TRAIS)		
		11. Contract or Grant No. DTRT12GUTC17		
12. Sponsoring Agency Name and Address US Department of Transportation Research and Special Programs Administration 400 7th Street SW Washington, DC 20509-0001		13. Type of Report and Period Covered Final Report: 6/1/2014 – 3/31/2017		
		14. Sponsoring Agency Code USDOT/RSPA/DIR-1		
15. Supplementary Notes:				

16. Abstract

The study develops two different eco-routing systems and uses them to investigate and quantify the system-wide impacts of implementing an eco-routing system. The first one is basically a Nash Equilibrium feedback system, which uses the Ant Colony optimization approach; Ant Colony based ECO-routing technique (ACO-ECO). The comparison shows that the enhanced ACO-ECO algorithm reduces the network-wide fuel consumption and CO_2 emission levels in the range of 2.3% to 6.0%, and reduces the average trip time by approximately 3.6% to 14.0% compared to the ECO-Subpopulation Feedback Assignment or ECO-SFA. The second developed eco-routing system is a system optimum eco-routing technique, the Linear Programming Feedback Eco-routing System (LPS-ECO), that can better utilize the road network resources. The LPS-ECO load-balances the traffic, so, it reduces the traffic congestion, consequently, minimizes the system wide fuel consumption and emission levels. The LPS-ECO is compared to the shortest-path-based eco-routing that is based on ECO-SFA. The comparison shows that for high traffic demands the LPS-ECO produces fuel consumption savings that reach 38%. LPS-ECO also produces savings in travel time in most of the cases. The study also developed a model to realistically simulate the eco-routing system in a connected vehicle environment and quantifies the impact of the communication performance on the eco-routing. The study shows that the communication can significantly affect the eco-routing system.

17. Key Words Eco-routing, connected vehicles, energy consumption, emission, multi-modal		18. Distribution Statement Unrestricted; Document is available to the public through the National Technical Information Service; Springfield, VT.		
19. Security Classif. (of this report) Unclassified	20. Security Classif. (of this page) Unclassified		21. No. of Pages #38	22. Price …

Form DOT F 1700.7 (8-72)　　　Reproduction of completed page authorized

TABLE OF CONTENTS

EXECUTIVE SUMMARY

The study develops two eco-routing systems and uses them to investigate and quantify the system-wide impacts of implementing an eco-routing system. In the first algorithm; the Ant Colony based ECO-routing technique (ACO-ECO), the study introduces and enhancement for the previous developments of the eco-rouing by utilizing the ant colony optimization. The enhancement improved the performance of the system in some cases such those experiences delayed updates or lack for updates due to severe congestions or a car blocking in cases of accidents. The study then conducts a simulation comparison to quantify the impact of this enhancement. The simulations show that the ACO-ECO algorithm and ECO-Subpopulation Feedback Assignment (ECO-SFA) have similar performances in normal cases. However, in the case of link blocking, the ACO-ECO algorithm reduces the network-wide fuel consumption and CO_2 emission levels in the range of 2.3% to 6.0%. It also reduces the average trip time by approximately 3.6% to 14.0%.

The study also developed a system optimum eco-routing technique, the Linear Programming Feedback Eco-routing System (LPS-ECO), that can better utilize the road network resources. The developed system utilizes the fuel consumption feedback and considers the road capacity along with the current traffic conditions to load-balance the traffic so as to reduce the traffic congestion, consequently, minimize the system wide fuel consumption and emission levels. LPS-ECO technique utilizes the linear programming to optimizes the network-wide fuel consumption. So, by using sufficient computation resources it can run in real time. The proposed system is compared to the shortest-path-based eco-routing that is based on ECO-SFA. The comparison shows that for high traffic demands the LPS-ECO produces fuel consumption savings that about 38%. LPS-ECO also produces savings in travel time in most of the cases.

Deploying this eco-routing system in the real network requires studying the impact of the communication network on its performance. Subsequently, the study developed a model to simulate the eco-routing system in the connected vehicle environment and quantifies the impact of the communication performance (in terms of packet drop rate and packet delay) on the eco-routing based navigation system. The simulation study shows that the communication can have significant impacts on the eco-routing system. Specifically, the simulation study shows that the errors due to data packet drops and delay are not significant. Consequently, the eco-routing algorithm is robust against drops and delay. However, the communication network setup (i.e, the allocation and the number of the roadside units) are important factors that affect the network-wide fuel consumption level.

This research effort resulted in the following peer-reviewed publications:

1. Ahn K. and Rakha H. (2014), "Eco-Lanes Applications: Preliminary Testing and Evaluation," Transportation Research Record: Journal of the Transportation Research Board, Issue 2427, pp. 41-53.
2. Wang J. and Rakha H. (2015), "Impact of Dynamic Route Information on Day-to-Day Driver Route Choice Behavior," Presented at the 94th Transportation Research Board Annual Meeting, Washington DC, January 11-15, CD-ROM [Paper # 15-4918].
3. Tawfik A. and Rakha H. (2015), "Modeling Heterogeneity of Driver Route Choice Behavior using Hierarchical Learning-Based Models: A Longitudinal, In-Situ Experiment in Real World Conditions," Presented at the 94th Transportation

Research Board Annual Meeting, Washington DC, January 11-15, CD-ROM [Paper # 15-3135].

4. Wang J., Rakha H. and Yu L. (2015), "Operating Mode Distribution Characteristics of Different Freeway Weaving Configurations and their Effects on Vehicular Emissions," Presented at the 94th Transportation Research Board Annual Meeting, Washington DC, January 11-15, CD-ROM [Paper # 15-1429].

5. Elbery A., Rakha H.A., ElNainay M., and Hoque M.A., (2015) "VNetIntSim: An Integrated Simulation Platform to Model Transportation and Communication Networks," International Conference on Vehicle Technology and Intelligent Transport Systems, Lisbon, Portugal, May 20-22.

6. Van Essen, M., Rakha, H., Vreeswijk, J., Wismans, L., & Van Berkum, E. (2015). "Day-to-day route choice modeling incorporating inertial behavior." IATBR Conference, 19-23 July, 2015, Windsor, UK.

7. Elbery A., Rakha H., El-Nainay M., Drira W., and Filali F., (2015), "Eco-Routing Using V2I Communication: System Evaluation," IEEE 18th International Conference on Intelligent Transportation Systems, Las Palmas de Gran Canaria, Spain, Sept. 15-18. [Paper # 1436].

8. Elbery A., Rakha H., ElNainay M., Drira W. and Felali F. (2016), "Eco-Routing: An Ant Colony Based Approach," 2nd International Conference on Vehicle Technology and Intelligent Transport Systems (VEHITS), Rome, April 23-24.

9. Elbery A., El-Nainay M. and Rakha H. (2016), "Proactive and Reactive Carpooling Recommendation System based on Spatiotemporal and Geosocial Data," WiMob, New York, USA, October 17-19.

10. Wang, J. and H.A. Rakha, *Fuel consumption model for heavy duty diesel trucks: Model development and testing.* Transportation Research Part D: Transport and Environment, 2017. **55**: p. 127-141.

11. Elbery, Ahmed, and Hesham A. Rakha. A Novel Stochastic Linear Programming Feedback Eco-routing Traffic Assignment System. No. 17-00912. 2017.

12. Elbery, Ahmed, and Hesham A. Rakha. A Scalable Framework for Modeling Communication in Vehicular Environment and An Application Case Study. Submitted to TRB 2018.

PROBLEM OVERVIEW

Currently, more than half of the world population are living in urban cities. The urban population is expected to continue to increase with the expectation that after about three decades, two out of three people will live in a city [1]. This continuous increase in urban population will result in numerous city problems. Currently several of these problems affect the human standard of living. These problems include scarcity of resources and increases in urban traffic congestion. The air pollution resulting from this traffic will also increase. Moreover, these traffic problems are anticipated to be tangled up in the infrastructure aging and deterioration [2]. Thus, the traffic problems and their consequences are major challenges facing cities and megacities of the future.

Among these challenges, one important major problem is the environmental and economic impact of the transportation sector. The importance of these problems is studied in many research efforts in the literature. For example, in 2008, the U.S. Department of Energy mentioned in [3] that approximately 30% of the fuel consumption in the U.S. is consumed by vehicles moving on the roadways. In addition, about one-third of the U.S. carbon dioxide (CO_2) emissions comes from vehicles [4]. The 2011 McKinsey Global Institute report estimated savings of "about $600 billion annually by 2020" in terms of fuel and time saved by helping vehicles avoid congestion and reduce idling at red lights or left turns. The statistics on the energy consumption since 1950 in the USA show that the transportation sector is the second consumer according to the U.S. Energy Information Administration [5]. The EIA reported in 2015 that the transportation sector consumes about 28% of the total energy consumed in the USA.

The U.S. Environmental Protection Agency reported that approximately 59% of the energy consumed by the transportation sector is consumed by light duty vehicles. It also reported that more than one-quarter of the total U.S. greenhouse gas emissions comes from the transportation sector. This fact makes transportation the second largest source of greenhouse gas emissions in the United States.

These statistics show the importance of addressing and optimizing the fuel consumption in transportation systems, not only because of the economic importance but also, and most importantly, because of the environmental impact of the transportation sector, which affects human health.

Eco-routing techniques are were proposed and studied in order to minimize the fuel consumption by assigning vehicles to the most environmentally friendly route. It was proposed in [6] where the authors presented a comprehensive study that provides optimal route choices for lowest fuel consumption. The fuel consumption measurements are made through the extensive deployment of sensing devices in the street network in the city of Lund, in Sweden. This study showed that about 46% of the trips were not made on the most fuel-efficient route. And approximately 8% of the fuel consumption could be saved on average using the most fuel-efficient routes. In [7] the authors combined sophisticated mobile-source energy and emission models with route minimization algorithms to develop navigation techniques that minimize energy consumption and pollutant emissions. They developed a set of cost functions that include the fuel consumption and the emission levels for the road links. Ahn and Rakha [8] showed the importance of route selection on the fuel consumption and environmental pollution reduction, by demonstrating through field tests that an emission and energy optimized traffic assignment could reduce CO_2 emissions by 14 to

18%, and fuel consumption by 17 to 25% over the standard user equilibrium and system optimum assignment. Later, Rakha et al. [9], introduced a stochastic, multi-class, dynamic traffic assignment framework for simulating Eco-routing using the INTEGRATION software [10]. They demonstrated that fuel savings of approximately 15% using two scenarios were achievable. In [11], the authors developed an Eco-routing navigation system that selects the fuel-efficient routes based on both historical and real-time traffic information.

In this study, we focused on these transportation problems, namely, the fuel consumption, pollutant emissions and the related parameters including congestion and traveler travel times. We developed two new eco-routing systems based on the feedback from the moving vehicles.

APPROACH AND METHODOLOGY

In order to quantify the system-wide impacts of eco-routing strategies, the study utilizes the INTEGRATION software [9, 10, 12, 13], which is a microscopic traffic assignment and simulation software. The INTEGRATION simulation model provides 10 basic user equilibrium traffic assignment/routing options. INTEGRATION supports 5 vehicle class, each has its own parameters and routing tree. One important feature of INTEGRATION is its support for eco-routing traffic assignment which tries to minimize the fuel consumption and emission levels by assigning vehicles the most environmentally friendly route. The INTEGRATION model updates the vehicle speed and location every decisecond based on a user-specified steady-state speed-spacing relationship along with the speed differential between the subject vehicle and the heading vehicle. INTEGRATION model uses the variable power vehicle dynamics model to estimate the vehicle's tractive force. Consequently, it implicitly accounts for gear-shifting on vehicle acceleration, which ensures realistic vehicle accelerations estimation. More specifically, the model computes the vehicle's tractive effort, aerodynamic, rolling, and grade-resistance forces, as described in detail in the literature[14, 15].

The following section describes the fuel consumption and emission models and the eco-routing algorithm implemented in the INTEGRATION software given that they are the two building blocks of the study.

Car Following model in INTEGRATION

Once the vehicle routes are selected, the INTEGRATION updates the vehicle longitudinal and lateral location (lane choice) every decisecond. The longitudinal motion of a vehicle is based on a user-specified steady-state speed-spacing relationship and the speed differential between the subject vehicle and the vehicle immediately ahead of it. In order to ensure realistic vehicle accelerations, the model uses a vehicle dynamics model that estimates the maximum vehicle acceleration level. Specifically, the model utilizes a variable power vehicle dynamics model to estimate the vehicle's tractive force that implicitly accounts for gear-shifting on vehicle acceleration. The model computes the vehicle's tractive effort, aerodynamic, rolling, and grade-resistance forces, as described in detail in the literature [14, 15]

In INTEGRATION, the car-following model computes the speed $u_{n(t+\Delta t)}$ of the following vehicle (n) at the new time step $t + \Delta t$ as [16]:

$$u_{n(t+\Delta t)} = min \left\{ \begin{array}{c} u_{n(t)} + a_n(t)\,\Delta t\,, \\ \dfrac{-c_1 + c_3 u_f + \bar{s}_n(t+\Delta t) - \sqrt{A}}{u_{n-1}(t+\Delta t)^2 + d_{max}\left(\bar{s}_n(t+\Delta t) - \dfrac{1}{k_j}\right)} \end{array} \right\} \qquad (1)$$

Where

$$A = \left[c_1 - c_3\,u_f\,\bar{s}_n(t+\Delta t)\right]^2 - 4c_3\left[\bar{s}_n(t+\Delta t)\,u_f - c_1\,u_f - c_2\right] \qquad (2)$$

and c_1, c_2, and c_3 are the model constants which are computed as:

$$c_1 = \frac{u_f}{k_j\,u_c^2}(2u_c - u_f); \qquad (3)$$

$$c_1 = \frac{u_f}{k_j\,u_c^2}(u_f - u_c)^2; \qquad (4)$$

$$c_3 = \frac{1}{q_c} - \frac{u_f}{k_j\,u_c^2} \qquad (5)$$

and the vehicle spacing is computed as:

$$\bar{s}_n(t+\Delta t) = x_{n-1}(t) - x_n(t) + \lfloor u_{n-1}(t) - u_n(t)\rfloor\Delta t + 0.5a_{n-1}(t+\Delta t)\Delta t^2 \qquad (6)$$

Here $a_n(t)$ is the acceleration of the vehicle n); u_f is the free-flow speed of the roadway; u_c is the roadway speed-at-capacity; q_c is the roadway capacity; k_j is the roadway jam density; $x_n(t)$ and $x_{n-1}(t)$ are the positions of the subject vehicle the lead vehicle at time t; d_{max} is the maximum acceptable deceleration level (m/s2). INTEGRATION also uses a validated lane selection and lane-changing logic [17].

Delay Calculation in INTEGRATION

Within the proposed model, the delay experienced by each individual vehicle (n) is computed for each traveled link (l) , as the difference between the vehicle's simulated travel time and the travel time that the vehicle would have experienced on the link at free speed as expressed [18]. And the total delay experienced by the subject vehicles is computed as:

$$D_n = \sum_{l \in vehicle\,Path} D_n^l = \sum_{l \in vehicle\,Path} \int_{t_0}^{t}\left(u_f - \frac{u(t)}{u_f}\right)dt \qquad (7)$$

Fuel Consumption and Emissions Estimation

Computing the fuel consumption and emission levels are imperative in any traffic modeler. The INTEGRATION software is capable of computing the second-by-second fuel consumed; vehicle emissions of carbon dioxide (CO2), carbon monoxide (CO), hydrocarbons (HC), oxides of nitrogen (NOx), and particulate matter (PM).

INTEGRATION uses the VT-Micro model that was described in details in [19]. It computes the second-by-second fuel consumption rate $\mathcal{F}(t)$ as:

$$
\mathcal{F}(t) = \begin{cases} exp\left(\displaystyle\sum_{i=1}^{3}\sum_{j=1}^{3} P_{i,j}^{+} \; u^i a^j\right) & if \; a \geq 0 \\[2em] exp\left(\displaystyle\sum_{i=1}^{3}\sum_{j=1}^{3} P_{i,j}^{-} \; u^i a^j\right) & if \; a < 0 \end{cases} \tag{8}
$$

where $P_{i,j}^{+}$ are model regression coefficients in case of acceleration at speed exponent i and acceleration exponent j; $P_{i,j}^{-}$ are model regression coefficients in case of deceleration at speed exponent i and acceleration exponent j; u is the instantaneous vehicle speed in km/h, and a is the instantaneous vehicle acceleration (km/h/s).

In our proposed modeler also, we have developed another fuel consumption model, the Virginia Tech Comprehensive Power-based Fuel consumption Model (VT-CPFM) [20]. The basic advantage of this model is that the fuel consumption cost of the links can be calculated for each vehicle types based on the vehicle parameters such as the rolling resistance, the frontal area, and engine efficiency. By using this model, different vehicle types can be assigned different routes at the same time.

Calculating Vehicle Stops

In the INTEGRATION model, the time resolution of the simulation enables the modeler to calculate the partial stops. Consequently, the total number of stops experienced by a vehicle on a link is computed as the sum of the partial stops incurred by the vehicle along that link [21]. The partial stop can be calculated for each vehicle as:

$$
S_i = \frac{u_{i-1} - u_i}{u_f} \qquad \forall \, u_i < u_{i-1} \tag{9}
$$

which is the ratio of the vehicle's instantaneous speed reduction over a one-second interval to the link free-speed.

We use the INTEGRATION framework to develop the new eco-routing systems as well as to develop the communication in vehicular environment. The following sections describe these systems in details.

ECO-ROUTING: AN ANT COLONY BASED APPROACH

We first study the Eco-routing performance and show that in some cases its performance may not be optimum. Subsequently, based on this, we propose an ant colony Eco-routing (ACO-ECO) [22] algorithm that employs the ant colony optimization algorithms [23]. Due to the major differences between the ant colony and the transportation network, the ant colony algorithms are not directly applied to select the best routes, however, they are used to optimize the route selection process by optimizing the route selection updating. Finally, we compare the proposed approach to the subpopulation feedback Eco-routing algorithm (SPF-ECO) [9].

Ant Colony Optimization

Ant colony optimization [23] is a branch of the larger field of swarm intelligence [24]. Swarm intelligence studies the behavioral patterns of social insects such as bees, termites, and ants in order to simulate these processes. Ant colony optimization is a meta-heuristic iterative technique inspired by the foraging behavior of some ant species. In the ant colony, ants walking to and from a food source deposit a substance called pheromone on the ground. In this way, ants mark the path to be followed by other members of the colony. The shorter the path, the higher the pheromone on that route, and consequently, the preferable this route is. The other ant colony members perceive the presence of pheromone and tend to follow paths where pheromone concentration is higher. Ant colony optimization exploits a similar mechanism for solving some optimization problems.

In this paper, we use the same ant colony concept to optimize the fuel consumption and emission cost for a transportation network. Vehicles are employed as artificial ants, the pheromone is considered to be the inverse of the fuel consumption cost for each link. Each artificial ant periodically deposits the pheromone by updating the fuel consumption cost for the link it is traversing.

There are many variants of ant colony optimization. However, all of them share the same idea described earlier. The main steps in each iteration are: 1) construct the solutions, 2) conduct an optional local search step, and 3) update pheromones. The ant colony system does not specify how these three steps are scheduled and synchronized, the system leaves these decisions to the algorithm designer [25]. In the solution construction step, artificial ants construct a feasible solution and add it to the solution space. The system starts with an empty solution space, the ants start at the nest, and each ant probabilistically chooses a solution e_i between a set of paths $\{e_1, e_2, \ldots e_k\}$ to reach the food source. To choose between these paths, each ant uses the probability P_i computed in Equation (10).

$$P_i = \frac{\varphi}{\sum_{j=1}^{k} \varphi_j}$$

(10)

Where φ_i is the amount of pheromone on path e_i. This probabilistic behavior for route selection guarantees the exploration of more feasible solutions and avoids converging to local ones.

The pheromone updating takes place while the ants are moving, where they deposit the pheromone on their paths. Also, as time passes, the pheromone evaporates based on an

---

evaporation factor ρ. Subsequently, after each iteration, the phenome is updated according to Equation (11).

$$\varphi_i = (1 - \rho)\,\varphi_i + \sum_{j=1}^{m} \Delta\varphi_j \qquad\qquad \textbf{(11)}$$

Where m is the number of ants that traverse a link, and $\Delta\varphi_j$ is the amount of pheromone deposited by ant j. After the solution construction and before the pheromone updating, the local search step can be carried out to improve the solution. This step is optional and problem specific.

In the proposed approach, we utilize these steps to achieve our objective of minimizing the fuel consumption and consequently the pollutant emissions.

Ant Colony Based Eco-routing (ACO-ECO)

This section presents the proposed approach (ACO-ECO) and describes its operation in details. In ACO-ECO, the ant colony techniques will be applied to optimize the fuel consumption and emissions in the transportation network. The vehicles are the artificial ants, and the pheromone is the inverse of the fuel consumption. Because of the major differences between the ant colony system and the transportation network, we introduce some variations to ant colony techniques to tailor it to the specific application. The ACO-ECO uses a number of steps that are described here.

Initialization

This phase initializes the cost associated with the various links. Because initially, the links are free, the cost of each link is initialized to the free flow speed fuel consumption using equation (8).

Route Construction

This phase starts directly after the initialization phase and is repeated periodically and was defined to be 60 seconds in this application. In this phase, the ACO-ECO builds the minimum path based on the cost of each link. When the vehicle leaves a route link, it searches the tree to find its next link.

The probabilistic route selection (introduced by Equation (10)) is an important mechanism in ant colony algorithms to search all the available routes. However, this mechanism as described in Equation (10) cannot be applied in vehicular route selection because it is not realistic. As mentioned earlier, drivers try to select routes that minimize their cost, while this probabilistic selection assigns a random route to each vehicle based on the route's pheromone level (route cost) relative to that for all other routes. Using this equation, and due to the randomness, a vehicle might be assigned a very high-cost route which is not realistic and is not consistent with the driver behavior when selecting routes. Consequently, it will result in a higher fuel consumption level. So, we use another technique to introduce some limited randomness into the route selection mechanism while maintaining the error within a given predefined margin. An error factor is configured for the network. This error

factor (α) is used to add some error to the cost of the links, subsequently to the tree building and the route selection algorithms. The error value added to the link cost is a randomly selected point from the standard normal distribution $N(0, \sigma)$, where σ is the standard deviation and $\sigma = \alpha \cdot link\_cost$. In this way, we have a grantee that 95.45% of the link costs are within $(1 \pm 2\alpha) \cdot link\_cost$. Which means that by controlling the error factor α we can control the randomness level within the route selection algorithm.

Pheromone Update

In this phase, two updating processes take place. Pheromone deposition where ants deposit pheromone to indirectly communicate the route preference to the following ants. And the pheromone evaporation, where the pheromone level on each link decays with time.

- ### *Pheromone Deposition*

In the vehicular network, each vehicle sends the cost it experienced on a link to the TMC, and consequently, the link cost is updated in the routing algorithm. In the SPF-ECO, the vehicles only submit the link cost when leaving the link. The advantage of this method is the small number of updates being sent on the network and consequently the low network overhead. But on the other hand, it results in delayed updates and fixed cost for empty or blocked links as mentioned earlier.

In contrast to the SPF-ECO, the ACO-ECO overcomes these issues by enabling vehicles to submit multiple updates while traveling the link. These updates can be sent periodically either time-based or distance-based. Using time-based updating, the vehicles have a predefined maximum updating interval T. The vehicles should send their estimation for the link cost each T seconds. This cost updating method can control the number of updates that are sent over the network. However, it has an important drawback; for low speed links or blocked links, the vehicles will send many unnecessary updates. Another drawback is for short length links and/or high speed links, this time interval T may be longer than the link traversal time. Consequently, no updates would be sent for these links. This drawback can be overcome by setting T to a value that is shorter than the minimum link travel time in the network, however, this will result in many unnecessary updates for long links or low speed links.

Another way to submit the link cost updates is the distance based updating, where the vehicles should submit an update every distance D it traverses on the link. In contrast to the time based updating, the distance based method limits the number of updates for each link. But on the other hand, for blocked links, the updates will not be sent and consequently, the cost will be fixed for blocked links resulting in the same problem as the SPF-ECO algorithm.

Consequently, a compromise approach is proposed, which combines both the time- and distance-based updating to take advantage of the merits of each approach. Also, we used the end of the link updating where the vehicle sends an update when it leaves the link. To estimate the link fuel consumption, the ACO-ECO algorithm defines the maximum time interval T and the maximum distance D to report conditions. When any of these conditions is met, the vehicle submits a new update quantifying its estimation for the overall link cost, and then resetting its time and distance counter. To calculate the fuel it consumed, the ACO-ECO

periodically estimates the fuel consumption rate using the VT-Micro model in Equation (8). And then uses Equation (12) to accumulate the total fuel consumed in the previous interval.

$$C = \sum_t F(t) \cdot \Delta t \qquad (12)$$

Where $F(t)$ is the VT-Micro model instantaneous fuel consumption rate, and Δt is the fuel consumption calculation interval which is typically 0.1 seconds in INTEGRATION. Whenever either T or D is reached, the ACO-ECO estimates the overall link fuel consumption C_l as shown in Equation (13).

$$C_l = \frac{C \cdot L}{d} \qquad (13)$$

Where d is the distance traveled in the previous period in meters $(d \leq D)$, and L is the link length in meters. This calculation assumes that the conditions on the remainder of the link will continue as was observed by the vehicle.

- *Pheromone Evaporation*

To overcome the fixed cost problem for empty links, the cost of these links must be updated when the TMC has not received updates for a period of time. In an ant colony, if no pheromone is deposited for a long time, the link pheromone level will decay towards zero due to the evaporation, this is an indication of the low preference for that route. In a transportation network, not receiving an update about a link for a long time, indicates that this link is empty. Consequently, the cost of this link must be updated toward the free flow speed cost (C_{ff_l}). So, in this case, the TMC updates the cost as follows. First, it finds the minimum updating interval (τ_l) for the link. This value is the minimum of three parameters; the updating interval (T), the link travel time at free-flow speed, and the updating interval in case of distance based updating. These parameters are shown in Equation (14). The rationale is that after receiving an update, the next vehicle will send an update in case of one of three situations; it reaches its updating interval T, it reaches its updating distance, or it ends the link.

$$\tau_l = min\left(T, \quad \frac{L_l}{S_{ff_l}}, \quad \frac{D}{S_{ff_l}}\right) \qquad (14)$$

Where T is the updating interval, D is the updating distance, L_l is the link length and S_{ff_l} is the free-flow speed of the link.

Subsequently, the ACO-ECO algorithm estimates the overall link cost C_l as shown in Equation (15). This evaporation technique results in exponential increasing or decreasing in the link cost towards the free-flow speed cost.

$$C_l = C_l - \frac{\Delta t}{\tau_l}\left(C_l - C_{ff_l}\right) \qquad (15)$$

Where C_{ff_l} is the free-flow speed fuel consumption estimate for the link, and Δt is the evaporation interval after which the evaporation process should be performed for the link cost if no updates were received.

Simulation Results

In this section, we compare the proposed approach ACO-ECO to the SPF-ECO for different traffic rates using the INTEGRATION software [10]. The network shown in Figure 1**Error! Reference source not found.** is used for comparing the two approaches.
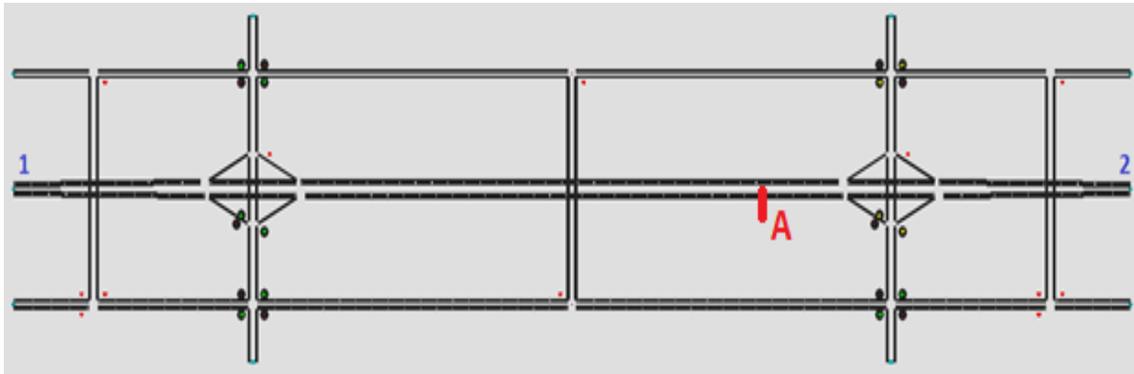
Figure 1. Road Network used in Simulation.

The network consists of 10 zones with the main highway (center horizontal road) between zone 1 and zone 2, and two arterial roads (side roads). The network size is 3.5 km x 1.5 km. The free-flow speeds are 110 and 60 km/h for the highway and arterial roads, respectively. The highway has 3 lanes in each direction while the other roads have only 2 lanes in each direction. Regarding the origin-destination traffic demands (O-D demands), we use 5 different scenarios, as shown in Table 1, Origin-Destination Traffic Demand. Configuration. . The main traffic stream is the traffic between zone 1 and 2 for each direction, the side traffic streams are between each two other zone pairs. This traffic rate is generated for half an hour, and the simulation runs for 4500 seconds to ensure that all the vehicles complete their trips.

Table 1. Origin-Destination Traffic Demand Configuration.

	Main Demand (Veh/h)	Secondary Demand (Veh/h)	Total no. vehicles (Veh)
1	500	50	1600
2	1000	75	2650
3	1500	100	3700
4	2000	125	4750
5	2500	150	5800

The comparison is done in two cases; the normal operation (no incident) case where there is no link blocking, and in the case of blocking due to an incident (link blocking case). For each case, we run each traffic assignment technique (ACO-ECO, and SPF-ECO) 20

times with different seeds to consider the output variability due to randomization. This is repeated for each of the five O-D demand configurations. The error factor is set for both techniques to 1%. For the ACO-ECO parameters, the maximum update interval T is 180 seconds, and the maximum update distance D is 750 meter.

Normal Operation Scenarios

For the normal operation scenarios, the results show no significant differences between the ACO-ECO and the SPF-ECO for average fuel consumption levels, as shown in Figure 2. The figure also shows that as the traffic demand increases, the average fuel consumption and the average trip time increases due to the higher congestion levels. Moreover, the results show the same behavior for the average trip time, the CO_2 and NO_x emissions levels, where ACO-ECO has no significant effect on any of them.
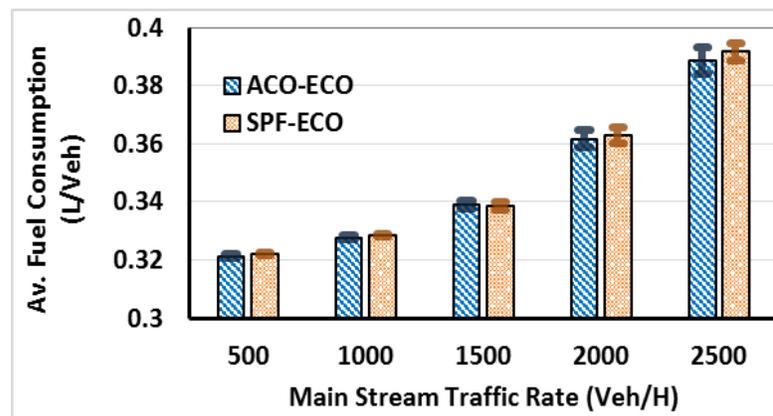

Figure 2.   Average Fuel Consumption (L/Veh).

Regarding the CO emission, the ACO-ECO has a higher emission level as shown in Figure 4.
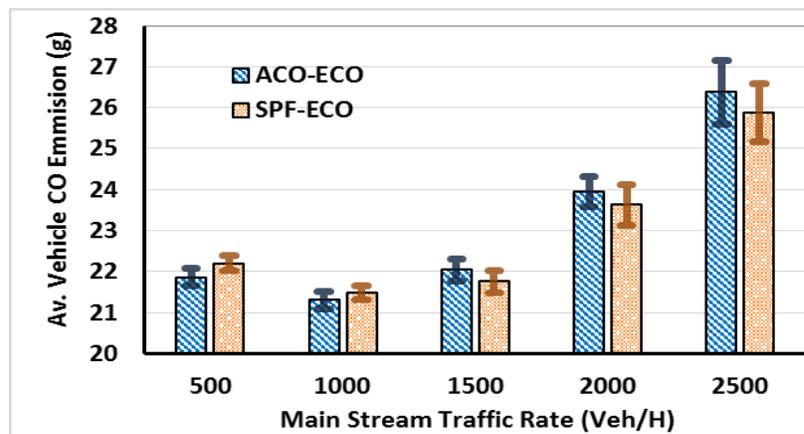
Figure 3. Average Vehicle CO Emission.

Incident Scenarios

To simulate the link blocking in the network, we configured an incident on the highway from zone 1 and 2 at point (A) marked in Figure 1, the incident does not affect the other direction from zone 2 to zone 1. This incident occurs 10 minutes after starting the simulation and blocks 50% of the highway (1.5 lanes) for 5 minutes. Then the blocking is reduced to 25% of the highway for the next 10 minutes, then the incident is completely removed and the highway works with its full capacity.

Figure 4 shows the fuel consumption in case of an incident. The figure demonstrates that the ACO-ECO algorithm reduces the average fuel consumption level for all traffic demands. The reduction ranges between 2.3% to 6% compared to the SPF-ECO.
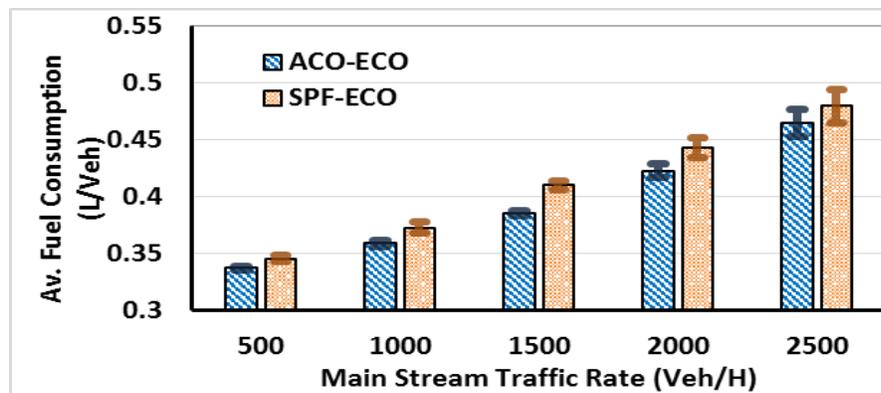

Figure 4. The Average Fuel for the Link Blocking Scenario.

These results show the ability of ACO-ECO to reduce the fuel consumption level and the trip time in addition to all the time-related measurements. ACO-ECO also succeeds in reducing the pollutant emissions in most cases.

Table 1 shows the percentage reduction attributed to the ACO-ECO for both fuel consumption, different emissions, and different time-related measurements. For instance, the fuel consumption is reduced by 6% in the moderate traffic scenario and this reduction ratio decreases as the traffic demand increases. This also applies for the CO_2 emissions and the time-related measurements. The reason is that as the traffic demand increases, the congestion increases and thus affects all the alternative routes, which limits the ACO-ECO ability to recover from the congestion.

Table 2   Percent of Reduction Made by ACO-ECO over SPF-ECO in case of Link Blocking

Traffic rate	Fuel	CO_2	CO	HC	NO_X	Trip time	Stop delay	Accel. noise	Accel./Decel. Delay
500	2.37	2.29	3.75	3.71	1.60	3.64	4.04	1.87	12.02
1000	3.72	3.86	1.05	1.73	0.91	8.83	19.04	4.90	21.97
1500	6.06	6.42	-1.51	0.38	0.24	14.98	27.68	5.28	25.43

| 2000 | 4.57 | 4.75 | 0.49 | 2.19 | 0.11 | 12.66 | 19.75 | 4.91 | 16.84 |
| 2500 | 3.09 | 3.32 | -2.10 | -0.58 | -0.75 | 7.11 | 15.39 | 1.61 | 11.34 |

To find the significance of the reduction made by ACO-ECO, analysis of variance (ANOVA) is employed to compare means of ACO-ECO to that of SPF-ECO.

The hypotheses are:-

- *Null hypothesis*: the means for both algorithms are equal ($H_0: \mu_1 = \mu_2$)
- *The alternate hypothesis*: the means are not equal ($H_a : \mu_1 \neq \mu_2$).

We applied this ANOVA for the fuel consumption results in the lowest traffic rate. Given this scenario has the lowest reduction in fuel consumption. The result shows that p-value is less than 0.0001. Which gives a strong evidence to reject the null hypothesis. And shows the significance of the reduction made by the ACO-ECO. And, since the lowest reduction level is significant, we can conclude that the higher levels for other configuration are also significant. Table 2 also, shows some rare cases where some emissions increase in due to the use of ACO-ECO. For instance, CO and NOx emissions increased in case high traffic rates.

SYSTEM OPTIMUM ECO-ROUTING USING LINEAR PROGRAMMING

This section introduces the proposed linear programming stochastic-based eco-routing technique (LPS-ECO) [26] that tries to minimize the network-wide fuel consumption by using all the available network resources (roads) toward the destination

The linear program should be formulated in a way that minimizes the fuel consumption and at the same time guarantees route continuity for each individual traffic flow from its source to its destination. The route continuity condition is achieved by using individual flow balance at each node, which will be described later. The flow balance at a given intermediate node means that the summation of the traffic entering that node equals that exiting it. The combination of the objective function and the individual flow balance at each node guarantees the route continuity.

Since we use individual flow balance, we define the link-flow assignment as the portion of each individual flow that should go through each link. Consequently, if the network has f flows and m links, the linear program calculates the f portion for each of the m links. Consequently, the total number of variables in the program will be $m \times f$. The number of variables is relatively large for large networks with a large number of traffic flows. The other way to guarantee the traffic balance at each node is to use the total flow balance. The total flow balance can reduce the number of variables in the linear program. However, it cannot guarantee the route continuity. Therefore, we have to use the individual flow balance method.

Based on this flow distribution, the vehicles are assigned routes stochastically considering their source and destination. The route assignment algorithm will be described later.

The Objective Function: Minimizing Total Cost

We formulated the linear program objective function as follows:

We begin with the network directed graph $G(N, L)$, where $N = \{i : i = 1 \ to \ n\}$ is the set of n nodes and $L = \{l_{i,j} : i, j \in N\}$ is the set of m directed links. The network has a set F of f concurrent flows, each of rate q^k (in vehicles per hour [veh/h]) where k is the flow identification number ($k = 1 \ to \ f$). The total flow rate passing through the directed link $l_{i,j} \in L$ from node i to node j is $q_{i,j}$. For each network flow k whose rate is q^k, every directed $l_{i,j} \in L$ is assigned a portion (or a sub-flow) of this flow rate equal to $q_{i,j}^k$ such that $0 \leq q_{i,j}^k \leq q_{i,j}$ and $0 \leq q_{i,j}^k \leq q^k$.

The total flow rate $q_{i,j}$ on link $l_{i,j}$ is the summation of all the sub-flows passing from node i to node j as in Equation (16).

$$q_{i,j} = \sum_{k=1}^{f} q_{i,j}^k \qquad (16)$$

Assuming that the fuel consumption cost for a vehicle that passes link $l_{i,j}$ is $C_{i,j}$, then the cost of all vehicles passing this link in the unit time is

$$C_{i,j}^{Total} = C_{i,j} \sum_{k=1}^{f} q_{i,j}^{k} \qquad (17)$$

The objective of the linear program is to minimize the total network cost during the unit time which is

$$inimize \sum_{i=1}^{n} \sum_{j=1}^{n} C_{i,j} \sum_{k=1}^{f} q_{i,j}^{k} \qquad (18)$$

Constraints

The program constraints are built to satisfy two conditions; the first is the route continuity that we mentioned above, and the second is that the link capacity constraint, that is the total flow on each link should not exceed its capacity.

The individual flow balance at each node and route continuity constraints:

The individual flow balance is formulated as follows. For each intermediate node i, and for each individual flow k, the summation of the sub-flows of the kth flow entering this i^{th} node must be equal to the summation of the sub-flow of the kth flow exiting this node, as shown in Equation (19).

$$\sum_{d=1}^{n} q_{i,d}^{k} - \sum_{s=1}^{n} q_{s,i}^{k} = 0 \qquad (19)$$

Equation (19) applies to an intermediate node. If the node i is a source or a destination node, then Equation (19) should include the flow rate q^{k}. For the source node that generates the kth flow with rate q^{k}, we assume there is a fictitious source sending q^{k} to it, and vice versa for the destination nodes. This type of constraint will build $n \times f$ constraints as shown in Equation (20).

$$\sum_{d=1}^{n} q_{i,d}^{k} - \sum_{s=1}^{n} q_{s,i}^{k} = \begin{cases} q^{k} & i \text{ is the source of } k \\ -q^{k} & i \text{ is the dest. of } k \\ 0 & \text{intermediate node} \end{cases} \qquad \forall\, i \in N;\; k \in F \qquad (20)$$

The link capacity constraints:

For each directed link $l_{i,j}$ with capacity $cap_{i,j}$ (veh/h), the total flow rate traversing it should not exceed the link capacity. The link capacity constraints will build m constraints, one for each link, as shown in Equation (21).

$$\sum_{k=1}^{f} q_{i,j}^k \leq cap_{i,j} \qquad\qquad \forall\, l_{i,j} \in L \qquad\qquad\qquad (21)$$

The total number of variables in the linear program is $m \times f$, and the total number of constraints is $n \times f + m$. The final linear program to solve the problem is:

$$minimize \sum_{i=1}^{n} \sum_{j=1}^{n} C_{i,j} \sum_{k=1}^{f} q_{i,j}^k$$

Subject to:

$$\sum_{d=1}^{n} q_{i,d}^k - \sum_{s=1}^{n} q_{s,i}^k = \begin{cases} -q^k & \text{if } i \text{ is the source of flow } k \\ q^k & \text{if } i \text{ is the destination of flow } k \\ 0 & \text{intermediate node} \end{cases} \qquad \forall\, i \in N, k$$
$$\in F,$$

$$\sum_{k=1}^{f} q_{i,j}^k \leq cap_{i,j} \qquad \forall\, l_{i,j} \in L\,,$$

$$q_{i,d}^k \geq 0$$

Calculating Link Fuel Consumption Cost

As mentioned earlier, the proposed model uses a feedback system to calculate the fuel consumption cost of each road link. In this system, every individual car calculates its fuel consumption for each road link it traverses. Once the car exits the link, it reports this link cost to the TMC, which uses the updated link cost information to recalculate the link cost periodically.

An important question arises here: which model should be used to calculate the vehicle's fuel consumption on each link? In the literature, several models have been developed to calculate fuel consumption and emission levels. These models can be classified into two classes: macroscopic models [27, 28] and microscopic models [29, 30]. In macroscopic models, the average link speeds are used to estimate the fuel consumption and emission levels for each link. This class is characterized by its simplicity but has a limited accuracy because it ignores the impact of speed and acceleration on fuel consumption levels. The microscopic models overcome this limitation by using a vehicle's instantaneous speed and acceleration to estimate the fuel consumption and emission levels. Consequently, microscopic models provide higher accuracy at the cost of model complexity.

To have an accurate estimation of the fuel consumption for each vehicle and subsequently for each link, we used the INTEGRATION software, which is a microscopic traffic assignment and simulation software [10]. INTEGRATION uses the VT-Micro model [29] to calculate the vehicle fuel consumption rate $\mathcal{F}(t)$ every second based on the vehicle's second-by-second speed and acceleration as shown in Equation (8) in the previous section.

When the vehicle leaves the link, it reports its fuel consumption on this link to the TMC. The TMC smooths the link cost based on its previous cost and the newly received update using exponential smoothing as shown in (21).

$$C_{i,j} = \alpha \ C_{i,j} + (1 - \alpha)\overline{C_{i,j}}$$ (22)

where $C_{i,j}$ is the current cost for the link $l_{i,j}$, $\overline{C_{i,j}}$ is the newly received cost update, and α is the smoothing factor, whose typical value is 0.8.

Calculating Link Capacities

The link capacities are a major factor in the proposed algorithm. Using these capacities in the linear program constraint enables the system to minimize the network congestion, thus improving network-wide performance. However, calculating the exact link capacity is a challenging task because of the different link control types and the dynamic conditions of the opposing links. For instance, estimating the capacity of yield-sign-controlled links is very challenging. The reason for this is that the actual capacity of such a link does not depend only on the configured link capacity and the number of lanes, but also on the number of opposing links, the traffic rate, and distribution of the traffic rate on each of those opposing links, which are stochastic factors.

In this paper, we simplify this problem by using the formula in Equation (23) for the link capacities:

$$cap_{i,j} = \ nlan_{i,j} \times \ s_{i,j} \ \times \ \delta - \overline{q_{i,j}}$$ (23)

where $s_{i,j}$ is the lane base saturation flow rate for link $l_{i,j}$, $nlan_{i,j}$ is the number of lanes on the link, $\overline{q_{i,j}}$ is the current flow rate traversing it, and δ is a capacity reduction parameter that depends on the link control method. We use typical values for δ as follows:

- For free links (no traffic controls), $\delta = 1$.
- For signalized links (controlled by a traffic signal), $= \frac{T_g}{T_c}$, which is the ratio between the signal green time T_g to the total cycle length T_c of the signal.
- For yield sign links, $\delta = 0.4$.
- For stop sign links, $\delta = 0.3$.

In this way, the linear program can consider the different link parameters that can affect the actual link capacity.

Vehicle Route Construction

After solving the linear program and finding the link-flow assignment, the system can build the vehicle routes. When a given vehicle enters the network, the algorithm constructs its route from the source to the destination stochastically as follows:

The system first finds the flow of this given vehicle, k. Starting with the vehicle's source node, node i, and using it as the current node, it finds the links out of this node, the link set $\check{L} = \{l_{i,j} : j \in N\}$. If a link $l_{i,j} \in \check{L}$ was assigned a sub-flow of the flow k equal to $q_{i,j}^k$, then this link $l_{i,j}$ can be added to the route of the vehicle with the probability p_j, as shown in Equation (24).

$$p_j = \frac{q_{i,j}^k}{\sum_{l_{i,d} \in \check{L}} q_{i,d}^k} \qquad \qquad \text{(24)}$$

where $q_{i,j}^k$ is the sub-flow of the kth flow assigned to the link $l_{i,j}$.

After adding the first link to the route, the system finds the end node of this link and then uses it as the current node. This process is repeated until reaching the vehicle's destination node. In this way, vehicles of the same flow (traveling from the same source to the same destination) can take different routes while keeping the network-wide cost minimized.

Updating Routing Information

Every dynamic routing technique updates the routing information periodically based on a predetermined time interval called the route updating interval. Changing the value for this updating interval may significantly influence the network output. The LPS-ECO updates the link-flow assignment every updating interval by recalculating the link capacities and flow rates, subsequently, rebuilds and resolves the linear program and updates the link-flow assignment. In this paper, we used an updating interval of 60 s.

Simulation and results

To evaluate the proposed LPS-ECO algorithm, we developed it in INTEGRATION software, which is a microscopic traffic assignment and simulation program [10]. INTEGRATION is capable of simulating vehicle mobility with a time granularity of 0.1 s, which allows detailed analyses of acceleration, deceleration, lane-changing movements, car-following behavior, and shock wave propagations of the vehicles in the road network. This detailed analysis enables a very accurate calculation of each vehicle's instantaneous speed and acceleration and, consequently, accurate calculation of the fuel consumption using the VT-Micro model.

We compared the performance of the proposed LPS-ECO algorithm to that of the shortest-path-based eco-routing used in Subpopulation Feedback Assignment ECO-routing (SFA-ECO) [9], which is already included in INTEGRATION. Both routing techniques use the VT-Micro model to calculate the link costs. The main differences between them are the optimization method and the route building techniques. SFA-ECO utilizes the shortest-path algorithm to minimize the fuel cost for each individual vehicle, while LPS-ECO uses linear programming as described earlier. Secondly, every updating interval (60 sec in this example), SFA-ECO uses the deterministic route for each source-destination pair, which is the lowest-

cost route, so all vehicles belonging to the same flow should follow the same route (if the link costs do not change). This contrasts with LPS-ECO, which uses the stochastic route building technique in which vehicles of the same flow can take different routes.

Simulation Network and Traffic Demands

The network shown in Figure 1was used for comparing LPS-ECO and the SFA-ECO. Regarding the origin-destination traffic demands (O-D demands), we used six different scenarios, as shown in Table 3. In each scenario, the traffic demand has two types of traffic flows; namely, main and secondary traffic flows. The main traffic demand is highway traffic, which produces two flows between Node 5 and Node 10, one in each direction. The secondary traffic flows are between the node pairs {1, 6}, {2, 7}, {3, 8} and {4, 9} in each direction, which results in eight traffic flows. The total demand is 10 traffic flows. In the base scenario (the highlighted row in Table 3), the main flow rate is 750 Vph in each direction, and the secondary flow rate is 125 Vph, and each of the 10 flows runs for 1,800 s, resulting in a total demand of 1,250 vehicles. The flow rates for the other five simulation scenarios were generated by scaling up the base scenario by a scaling factor as shown in Table 3.

Table 3 O-D Traffic Demand Configuration

No.	Scale Factor	Main Demand (Veh/h)	Secondary Demand (Veh/h)	Total No. of Vehicles
1	1	750	125	1,250
2	2	1,500	250	2,500
3	4	3,000	500	5,000
4	6	4,500	750	7,500
5	8	6,000	100	10,000
6	10	7,500	1,250	12,500

In the simulation, the updating interval for both algorithms was set to 60 s. To have statistically accurate results, we ran each simulation scenario 20 times with different seeds. The results shown here are the averages of the 20 runs.

In order to make sure that all the vehicles are cleared, and thus the result among the two algorithms are comparable for each scenario, the network is configured to run for 3600 s (1 hour) which gives it enough time to clear all the vehicles.

Simulation Results

Figure 5 shows the fuel consumption for both SFA-ECO and LPS-ECO in addition to the fuel savings achieved by the LPS-ECO relative to the SFA-ECO for the six traffic scenarios shown in Table 3. The figure shows that for low traffic demand (scaling factors 1, 2) the differences between the two algorithms are very small. As the traffic demand increases, LPS-ECO shows a significant reduction in fuel consumption compared with SFA-ECO. LPS-ECO can save up to 38% of the fuel consumed in case of Scenario 5.
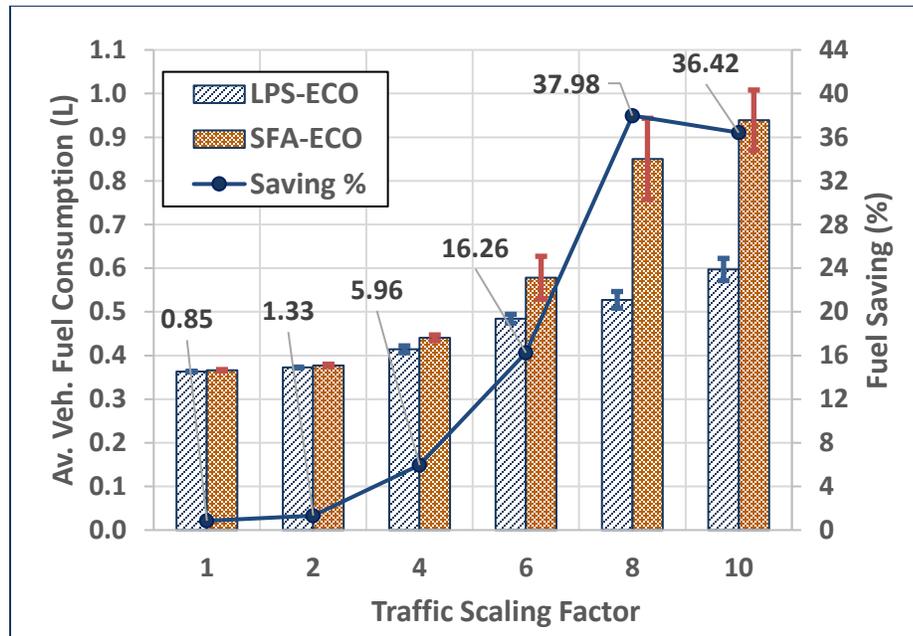
Figure 5. Fuel consumption for SFA-ECO and LPS-ECO for 60 s updating interval.

More interestingly, the average travel time results show that the LPS-ECO significantly reduced the average vehicle travel time. Figure 6 shows up to a 62% reduction in the case of high traffic demand levels. For low-traffic scenarios, the differences are not significant.
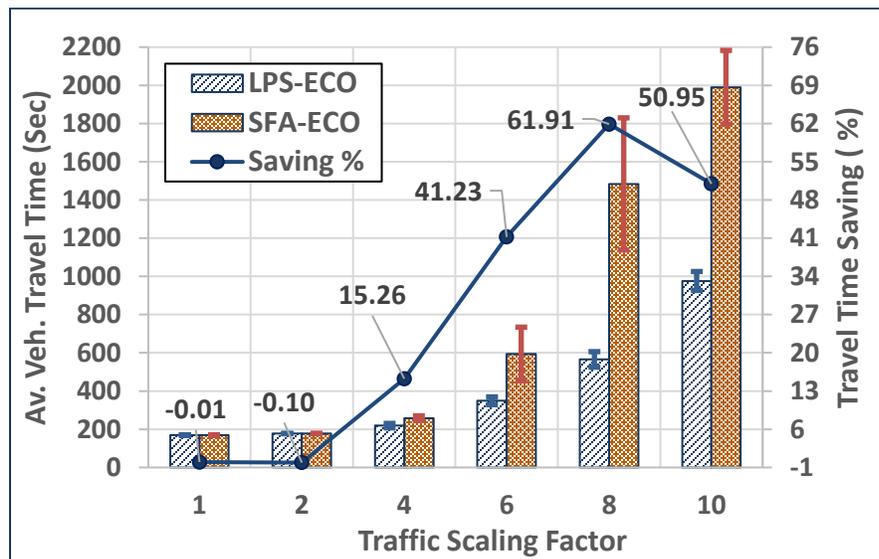
Figure 6. Average travel time for SFA-ECO and LPS-ECO for 60 s updating interval.

Figure 7 shows the impact of the routing algorithms on the main traffic streams (highway traffic flows between Nodes 5 and 10). It shows the time-space diagram for the main traffic demand for a 1% uniformly selected sample of the vehicles in both the LPS-ECO and SFA-ECO cases.

The figure shows that in the case of the shortest-path algorithm, many vehicles from the main traffic flow experienced congestion on the highway for a long time. In the case of LPS-ECO, there are small deviations from the highway free-flow speed, and vehicle trajectories show much smoother mobility on the highway. It also shows that in the case of LPS-ECO all the vehicles in the main traffic demand finished their trips around 400 s earlier.
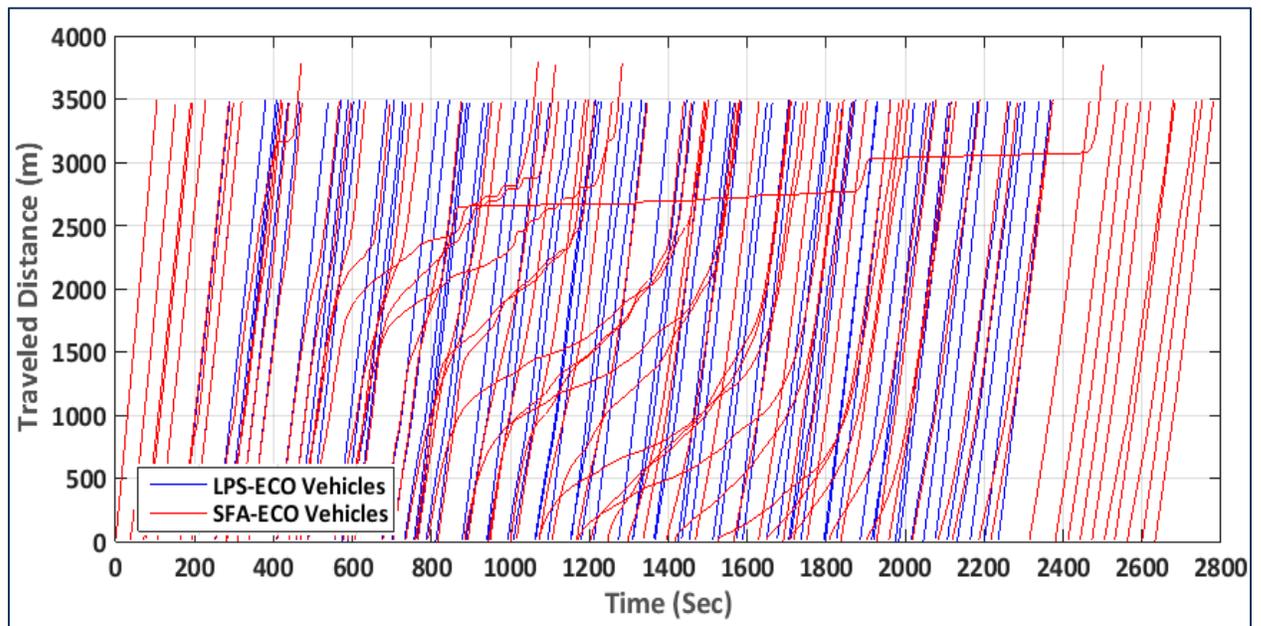
Figure 7. Time-space diagram for 1% sample of main traffic demand vehicles for both LPS-ECO and SFA-ECO.

ECO-ROUTING USING V2I COMMUNICATION: SYSTEM EVALUATION

In real deployment, eco-routing algorithms utilize the communication network to transfer the information between the vehicles and the TMC. Vehicular networks, Vehicle-to-vehicle (V2V) and vehicle to infrastructure (V2I), are promising communication technologies that are expected to represent the communication infrastructure for such applications. Consequently, V2V and V2I are key components in this system. Which means that the communication performance and parameters such as end-to-end delay and packet drop ratio should be considered when studying eco-routing systems since these communication parameters can affect the eco-routing system performance. In this section, the study investigates the impact of the communication network performance on the eco-routing system.

To achieve this purpose, the study first develops the VNetIntSim; a realistic platform for modeling and simulation of vehicular networks [31]. This modeler that is capable of simulating the communication networks in vehicular environments. Then this model is used to study the impact of the communication on the eco-routing.

The following subsections provide a brief introduction and literature review Vehicular ad-hoc networks. Then, describe the system model. Finally, the simulation results for different network scenarios are presented.

Vehicular Ad-hoc Network

Vehicular ad-hoc networks (VANETs) provide moving vehicles the capability to communicate with each other (V2V), or with roadside units (RSUs) forming a V2I network. Both communication types use a Dedicated Short Range Communication (DSRC) system. DSRC is standardized by 802.11p standards, which is essentially an amended version of IEEE802.11a for low overhead operation. Subsequently, IEEE standardized the entire communication stack using the 1609 family of standards known as Wireless Access in Vehicular Environments (WAVE) [32, 33]. DSRC spectrum is 75 MHz assigned by the U.S. Federal Communication Commission to the V2X communication. This spectrum is divided into seven 10MHz wide channels. As shown in Figure 8.
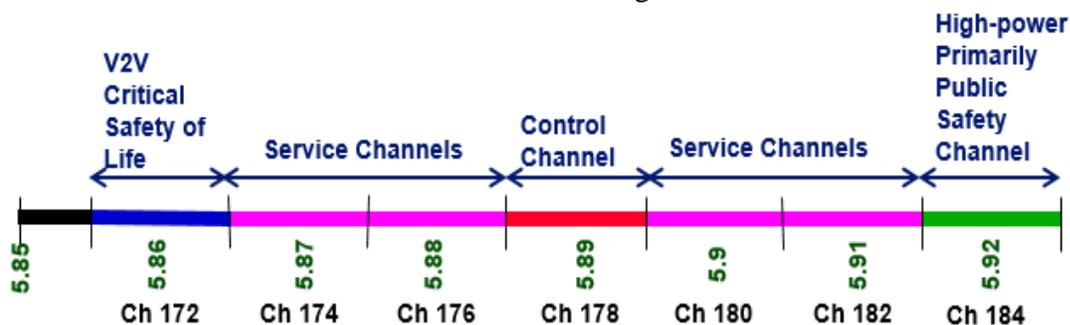

Figure 8. DSRC channels in U.S.

The middle channel (Ch. 178) is the control channel (CCH), which is generally restricted to safety communications only. The two edge channels are reserved for special

uses. The remaining four channels are service channels and are available for both safety and non-safety uses [34].

Varieties of applications are based on VANET communications. The safety applications are the primary category of these applications, where safety information are disseminated for the purpose of accident prevention in order to save people's lives [35-38]. In addition, post-accident investigation and traffic jam information can be exchanged to mitigate the effect of accidents. Other types of information can be exchanged in VANET including non-safety information such as cooperative driving applications [39, 40]; and road traffic congestion detection and management systems [41-43].

Eco-routing information (fuel consumption costs of the route) can be exchanged in VANET in order to select the best route for a trip. These costs are used as a route metric and the vehicles are assigned the routes that minimize their fuel consumption. In this study, we use the proactive data collection mechanism [44] where vehicles send the cost function when leaving a link.

System Model

To accurately model the moving vehicles and their communication we integrate the INTEGRATION traffic assignment and simulation software [9, 10] with the OPNET software [45] to build VNetIntSim. This integration enables to fully and accurately model V2V and V2I communications as well as vehicle mobility statistics more realistically. The main idea behind this integration is to use the advantages of both the INTEGRATION and OPNET platforms by establishing a two-way communication channel between them. This channel is used to communicate the required information between the two simulators including vehicle locations. These locations are modeled in INTEGRATION every decisecond and sent to the OPNET modeler, which updates the vehicle locations while they are communicating.

Simulation Architecture

INTEGRATION Software: The previous sections gave an overview about the INTEGRATION software.
OPNET Modeler: OPNET is a powerful simulation tool for specification, simulation, and analysis of data and communication networks. OPNET combines the finite state machines and analytical model. The most important OPNET characteristic is that has detailed tested implementations for many standard protocols covers the network layers.

The integration of the two software is shown in Figure 9. The communication module in each modeler is responsible for communicating the required information with the other side. In OPNET, the driver module is responsible for moving vehicles as well as triggering vehicles to take the appropriate reactions when receiving specific information. For example, when the driver receives a command from the INTEGRATION modeler that a vehicle passed a road link, the driver modules send this information to the specified vehicle and trigger it to send an eco-routing message to the TMC.
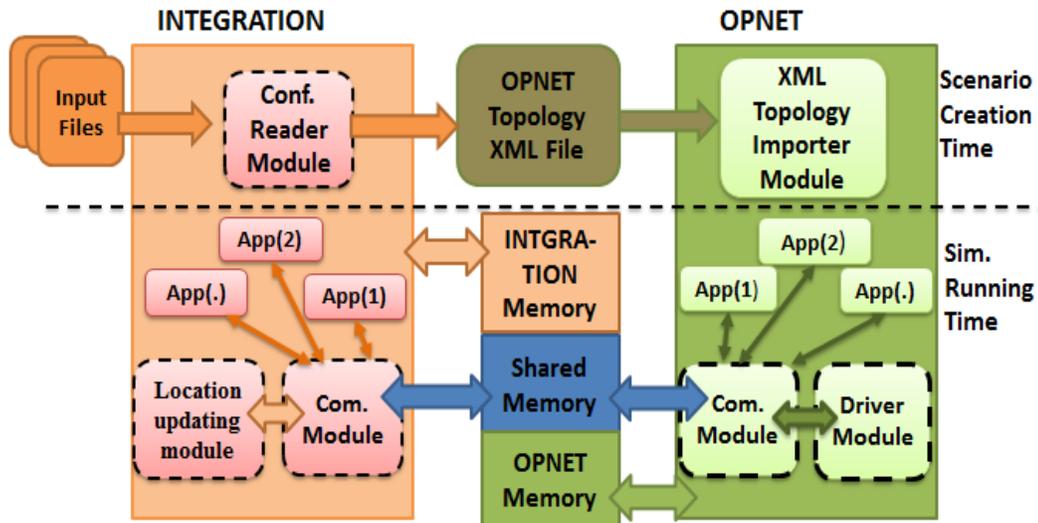
Figure 9. Architecture for integration OPNET and INTEGRATION

Eco Routing Models in OPNET

In OPNET, we developed two eco-routing sub-modules; one for the vehicles and one for the TMC. Both of them work over UDP protocol. The use of UDP avoids the overhead imposed by the TCP protocol as the vehicles send only one message for each link they traverse. The finite state machine (FSM) of the vehicle's eco-routing process sub-module is shown in **Error! Reference source not found.**. It has two initialization phases; the first (Init0) forces the process to wait until the lower layer protocols initialize; the second (Init) initializes the required state variables such as the TMC IP address, the port number, and the required statistics. After initialization, the process moves directly to the Idle state where it waits for an interrupt from the driver process to send the eco-routing message. The driver process is responsible for periodically communicating to the INTEGRATION software through the communication module. When it receives an eco-routing command from INTEGRATION, it sends an interrupt to the eco-routing module in the specified vehicle. This interrupt includes the Vehicle ID, link ID, the fuel consumption level on the link and the time when the vehicle passed this link. Whenever the eco-routing process receives an eco-routing interrupt, it promptly sends an eco-routing message to the TMC IP address and then returns back to an idle state.
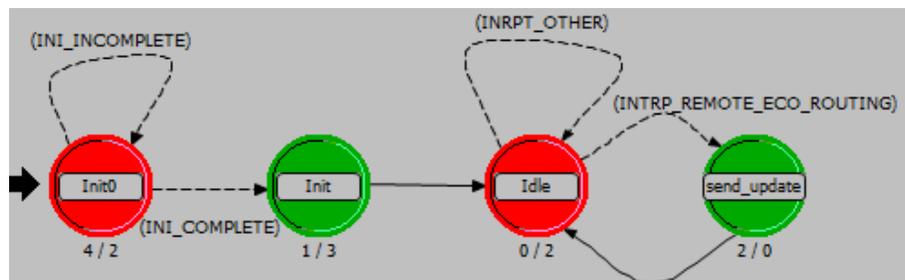
Figure 10. The vehicle's eco-routing process FSM

The eco-routing message format is shown in Figure 11. The sequence number of the message is used by the TMC to avoid processing duplicated messages. The time field enables the TMC to neglect the obsolete information.

The TMC eco-routing process receives these messages, store the received information, and send this information every decisecond to the communication module that will pass it to the INTEGRATION which in its turn update the routing information and assign the best routes to the vehicles.

In this modeler, we did not consider the communication from the TMC to the vehicles in order to assign the routes to them. We assume that the drivers use a Web interface that shows the best routes, and that the driver follows the TMC recommendations. The driver needs the routes to be updated when approaching intersections, where the vehicle is indeed connected to the TMC because we install the RSU, at intersections (as shown in Section IV). This means that the driver will the latest routing updates when he needs to make a decision.

0	8	16	24	32	40	48	56
Code							
Seq_Num				VehicleID			
LinkID				Cost1 (Fuel Consumption)			
Cost2 (Not used)				X (Vehicle's X Coordinate)			
Y (Vehicle's Y coordinate)				Time			

Figure 11. Eco-routing message format

Simulation Setup and Results

The road network shown in Figure 1 is used to test the eco-routing system. The traffic between the zones 5 and 10 is 1500 Veh/h for each direction. And for all other zone-pairs, it is 100 Veh/h. These traffic rates continue for half an hour resulting in 3700 vehicle trips. The simulations were run for a complete hour to make sure that all vehicles reach their destinations.

Regarding the communication setup, we used the infrastructure based VANET (V2I). Where the roadside units (RSUs) are located at all signalized intersections resulting in six RSUs. The RSUs were located at intersections for three reasons. First, these intersections are surrounded by link ends, therefore, it provides the best location to collect eco-routing messages. Second, since these intersections have signal controllers, they have the required infrastructure for connecting the RSUs to the traffic management center. Finally, the vehicles need to be connected to the TMC when approaching the intersections (decision points) to get the latest routing updates.

The RSUs are connected to a switch that connects them to the TMC server. The wireless interfaces are configured to use Orthogonal Frequency Division Multiplexing OFDM (802.11a) which is the base for the WAVE. We use channel 174 (5.86 GHz) with a 12 Mbps data rate. We use transmission power levels of 0.001, 0.005, 0.010 and 0.019 watt.

These power levels cover the range from Wi-Fi to DSRC (from 200 meters up to 1000 meters).

The RSUs are typically access points. Consequently, when a vehicle has a message to send, it waits until it becomes in the communication range of one of the RSUs. This means that the packets are being stored and forwarded. Thus, the packet end-to-end delay depends on the location where it was generated. If it was generated near an RSU, then the delay will be very small, and vice versa. This behavior is shown in Figure 12 for three transmission power levels. It shows that, as the transmission power increases, the average end-to-end delay decreases. The reason behind the multimodal distribution is that the eco-routing packets are generated at a fixed set of locations (the ends of links). So, for low power scenarios, more packets are generated in locations that are out of the communication range. This is reflected in more peaks for lower power scenarios.
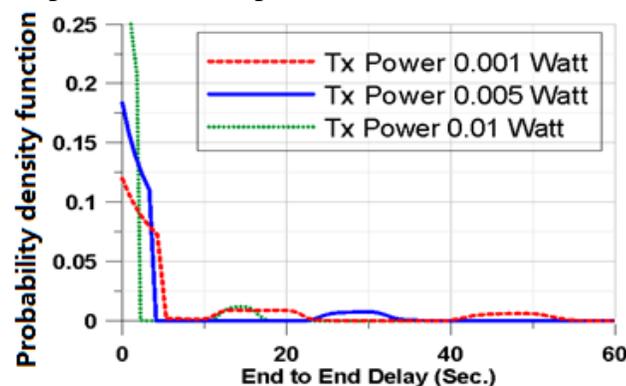
Figure 12. Probability density function (PDF) of the end-to-end delay

Effect of Packet Drops

Introducing the communication network into the eco-routing has two primary factors; the packet drops and the end-to-end delay. These two factors are expected to affect the performance of the applications. The packet drops will result in missing some information about the current links' states. Consequently inaccurate route fuel consumption calculations. Therefore, packet drops will result in errors in the route assignments. However, these errors not necessarily lead to higher fuel consumption. It depends on which links whose information are dropped, and the value of this information relative to the others.

Figure 13 compares the average vehicle fuel consumption (L/Veh) for different transmission power levels, and for 0% and 20% error factors in the eco-routing calculations. The "Direct ER" uses eco-routing without introducing the communication, while the "Com. ER" scenarios are the communication-based ER where the communication is introduced.

First, it shows that the eco-routing producing network-wide fuel savings in the range of 8%. This saves about 120 liters for this one hour of simulation. It also shows a small difference between the Direct ER and Communication-Based ER scenarios. The difference between them is generally inversely proportional to the transmission power; i.e. as the transmission power increases, the difference decreases. This is logical, because, as the transmission power increases, the number of packet losses decreases due to the wide

coverage, as shown in Table 4 which shows the average packets sent, packets received and packet drop ratio. Each row represents the averages of four simulation runs.

An important question relates to the significance of the changes introduced by the communication effects. Since the largest difference occurs for the lowest power, we compare the lowest power scenario for the communication-based ER to the direct ER using the analysis of variance (ANOVA) to check if these differences are significant. So, we first run each scenario ten times with different seeds. And then, ANOVA is used to compare the means, with the null hypothesis (H_0: $\mu_1 = \mu_2$) and the alternate hypothesis $H_a : \mu_1 \neq \mu_2$. The result shows that the p-value is $0.06 > 0.05$. Thus, there is no enough evidence to reject the null hypothesis. Subsequently, the differences introduced by the communication network are not significant.
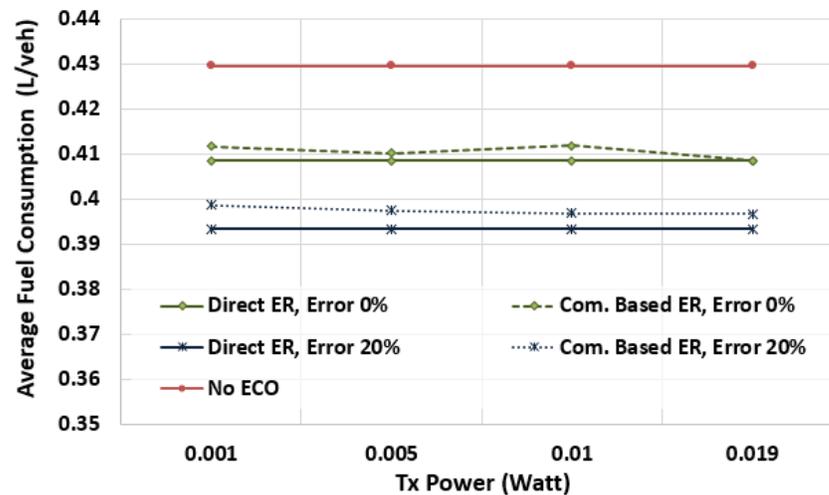

Figure 13. The effect of transmission power on the average Fuel consumption

Table 4. The drop ratio vs the transmission power

Tx Power	Packets Sent	Packets Received	Drop Rate
0.001	18,675	13,778	26.22
0.005	18,582	14,644	21.19
0.01	18,672	18,268	2.17
0.019	18,734	18,506	1.22

End-to-end Delay and its Effect

Figure 14 shows the packet end-to-end delay for the 0.001watt power level for two error factors. The end-to-end delay reflects the average speed in the network. The long end-to-end delay after 2000 seconds is due to the congestion on the highway that results in reducing the speed. Subsequently, the packets are stored for a longer time until the vehicles enter the RSU communication range.
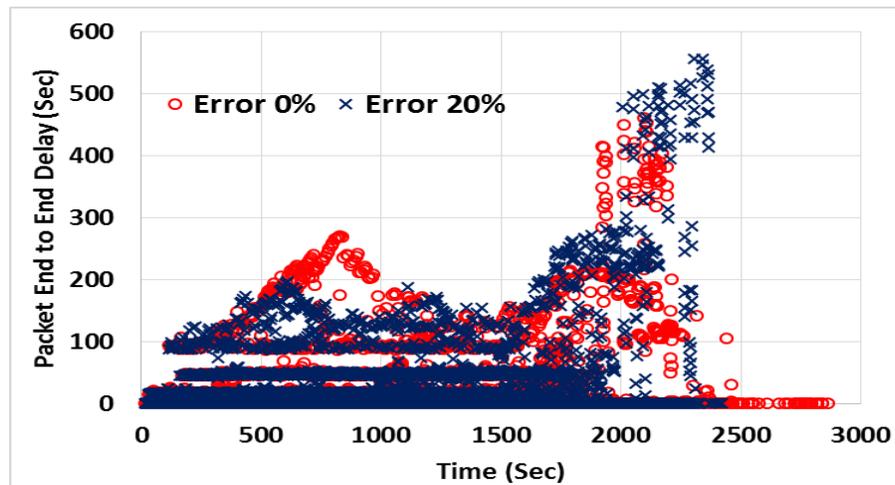
Figure 14. Packet end-to-end delay for Tx power 0.001 watt

In the previous scenarios, the TMC processes all the packets it receives without considering the packet delay. However, some packets are delayed for about 500 seconds such as shown in Figure 14. And consequently, the information it carries might be obsolete and does not describe the current link's state. To investigate the effect of the packet delay, we configured the TMC to discard the packets whose delay is greater than a specific time interval (allowable packet delay). We set this allowable delay to 60 seconds and run the same scenarios for different power levels.

After discarding the delayed packets, the result shows an insignificant difference.

Effect of RSU Locations

The location of the RSUs, in addition to the power levels, determine which link packets will be received, which link packets will be delayed or not received at all. To find the effect of the locations we use the same network but with only two RSUs. We compare two 2-RSU scenarios. In the first (HW scenario), the two RSUs are located on the highway at interchanges B and E shown in Figure 1. While in the second (AR scenario), the two RSUs are located on the arterial roads at intersections A and F.

The result shows that the locations of the RSUs result in significant changes in the case of lowest power level (0.001 watts) only. While for the higher power levels (0.005, 0.01, 0.19 watt), the effect of the locations is insignificant, as shown in Figure 15.

We again used ANOVA to find the significance of changes. For the lowest power level, the p-value is less than 0.0001, which provides strong evidence that the changes due to the RSU locations are significant. While for the 0.005 watts scenario, the p-value is 0.606. Which indicates the non-significance of the locations in case of high power scenarios.
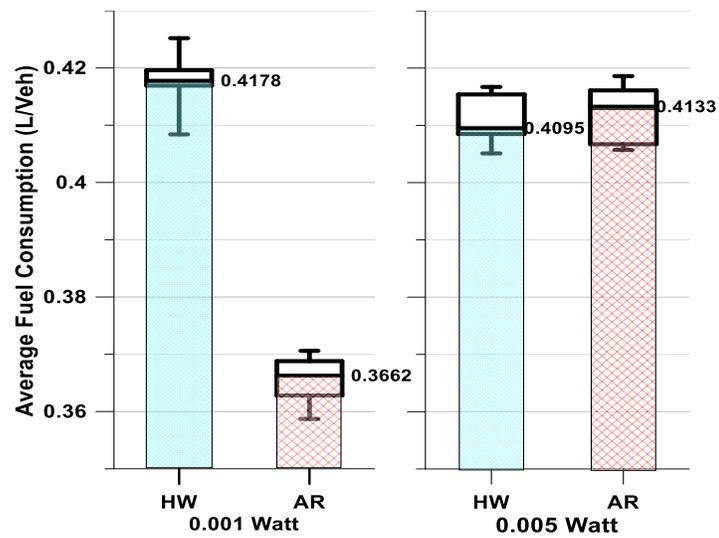
Figure 15. Fuel consumption Box-Whisker plots for 2RSU on the arterial roads scenarios for 0.001 and 0.005 power levels

CONCLUSIONS AND RECOMMENDATIONS

The study develops two eco-routing strategies. Ant Colony based eco-routing (ACO-ECO) which is a user equilibrium model. And the Linear programming Stochastic eco-routing which is a system optimum model. The study also develops a model to study the realistic deployment of the eco-routing systems by considering the impact of the communication network performance and setup on the eco-routing system performance. The study also conducts an extensive simulation and statistical analysis for the simulation outputs.

The simulations show that the ACO-ECO algorithm and ECO-Subpopulation Feedback Assignment (ECO-SFA) have similar performances in normal cases. However, in the case of link blocking, the ACO-ECO algorithm reduces the network-wide fuel consumption and CO2 emission levels in the range of 2.3% to 6.0%. It also reduces the average trip time by approximately 3.6% to 14.0%. the reason is that during the normal operation the updates sent from the vehicles are continuous because there is no link blocking. While, in the case of blocking the roads (i.e., due to incidents) the traditional eco-routing does not update the TMC. Which means the TMC database does not accurately represent the network state. While in the case of the ACO-ECO, the vehicles periodically estimate the link costs and update the TMC, which makes its database always up-to-date. So, it is important in the real deployment of the eco-routing to consider the cases in which there is link blocking as well as the empty links.

The main conclusion from the ACO-ECO is that in case of accedents or severe congestions, the eco-routing database at the TMC must be must be updated more frequently inorder to minimize the fuel consumption. These frequent updates are necceacry for the bloked or highly congested roads.

The second model developed in this study is the Linear programming Stochastic eco-routing (LPS-ECO). This model is a system optimum that attempts to route the vehicles in such a way that achieves the system optimum fuel consumption. The study compared the results of the LPS-ECO to the deterministic shortest path eco-routing technique. The results show that the LPS-ECO can achieve fuel consumption saving around 38% in case of high congested networks. It also shows that in most of the cases the LPS-ECO decreases the average trip time. The deep investigation of the simulation output shows that the cars move more smoothly in the case of LPS-ECO. The reason is that the LPS-ECO does not only consider the fuel consumption when finding the routes, but it also considers the road capacity. Which means it also tries to avoid the traffic congestion by utilizing the network resources and load-balancing the traffic.

The study also demoestrated that the deployment of system optimum technique (LPS-ECO) requires higher cost computational systems to satisfy it computation requirements. But the benefits of utilizing system optimum approatch worths the cost needed for these computational requirements.

The study also investigated the impact of the communication network performance on the eco-routing. The results show that the eco-routing is robust against packet drop and delays if there is a good coverage of overall the network. it also demonstrated the importance of the RSUs allocation. If the allocation of the RSUs does not cover the overall network, this may result in significantly increasing the system wide fuel consumption and emission levels.

REFERENCES

1.   UNFPA, *technical report: State of World Population 2011: People and Possibilities in a World of 7 Billion*, N.Y.U.N.P. Fund, Editor. 2011.
2.   Chourabi, H., et al. *Understanding Smart Cities: An Integrative Framework*. in *System Science (HICSS), 2012 45th Hawaii International Conference on*. 2012.
3.   U.S. Dept. Energy, *Annual Energy Outlook 2008, With Projection to 2030,*, in *Energy Inf. Admin., Washington, DC, Rep. DOE/EIA-0383(2008),* . 2008.
4.   U.S. Environ Protection Agency, *Inventory of U.S. greenhouse gas emissions and sinks*, in *1990–2006, Washington, DC,* . 2006.
5.   EIA, U.S. http://www.eia.gov/totalenergy/data/monthly/index.cfm#consumption. 2015.
6.   Ericsson, E., H. Larsson, and K. Brundell-Freij, *Optimizing route choice for lowest fuel consumption – Potential effects of a new driver support tool.* Transportation Research Part C: Emerging Technologies, 2006. **14**(6): p. 369-383.
7.   Barth, M., K. Boriboonsomsin, and A. Vu. *Environmentally-friendly navigation*. in *Intelligent Transportation Systems Conference, 2007. ITSC 2007. IEEE*. 2007. IEEE.
8.   Ahn, K. and H. Rakha. *Field evaluation of energy and environmental impacts of driver route choice decisions*. in *Intelligent Transportation Systems Conference, 2007. ITSC 2007. IEEE*. 2007. IEEE.
9.   Rakha, H., K. Ahn, and K. Moran, *INTEGRATION Framework for Modeling Eco-routing Strategies: Logic and Preliminary Results.* International Journal of Transportation Science and Technology, 2012. **1**(3): p. 259-274.
10.   Rakha, H., *INTEGRATION Rel. 2.40 for Windows - User's Guide, Volume I: Fundamental Model Features*, in https://sites.google.com/a/vt.edu/hrakha/. Last Access Feb. 2016.
11.   Boriboonsomsin, K., et al., *Eco-Routing Navigation System Based on Multisource Historical and Real-Time Traffic Information.* Intelligent Transportation Systems, IEEE Transactions on, 2012. **13**(4): p. 1694-1704.
12.   Ahn, K. and H. Rakha, *The effects of route choice decisions on vehicle energy consumption and emissions.* Transportation Research Part D: Transport and Environment, 2008. **13**(3): p. 151-167.
13.   Van Aerde, M. and S. Yagar, *Dynamic integrated freeway/traffic signal networks: A routing-based modelling approach.* Transportation Research Part A: General, 1988. **22**(6): p. 445-453.
14.   Rakha, H., et al., *Vehicle dynamics model for predicting maximum truck acceleration levels.* Journal of transportation engineering, 2001. **127**(5): p. 418-425.
15.   Rakha, H. and I. Lucic, *Variable power vehicle dynamics model for estimating truck accelerations.* Journal of transportation engineering, 2002. **128**(5): p. 412-419.
16.   Rakha, H.A., K. Ahn, and K. Moran, *Integration framework for modeling eco-routing strategies: Logic and preliminary results.* International Journal of Transportation Science and Technology, 2012. **1**(3): p. 259-274.
17.   Ahn, K., H.A. Rakha, and K. Moran. *System-wide impacts of eco-routing strategies on large-scale networks*. in *Transportation Research Board 91st Annual Meeting*. 2012.

18.   Dion, F., H. Rakha, and Y.-S. Kang, *Comparison of delay estimates at under-saturated and over-saturated pre-timed signalized intersections.* Transportation Research Part B: Methodological, 2004. **38**(2): p. 99-122.

19.   Rakha, H., K. Ahn, and A. Trani, *Development of VT-Micro model for estimating hot stabilized light duty vehicle and truck emissions.* Transportation Research Part D: Transport and Environment, 2004. **9**(1): p. 49-74.

20.   Rakha, H.A., et al., *Virginia tech comprehensive power-based fuel consumption model: Model development and testing.* Transportation Research Part D: Transport and Environment, 2011. **16**(7): p. 492-503.

21.   Rakha, H., Y.-S. Kang, and F. Dion, *Estimating vehicle stops at undersaturated and oversaturated fixed-time signalized intersections.* Transportation Research Record: Journal of the Transportation Research Board, 2001(1776): p. 128-137.

22.   Elbery, A., et al. *Eco-routing: An Ant Colony based Approach.* in *VEHITS*. 2016.

23.   Dorigo, M. and M. Birattari, *Ant Colony Optimization*, in *Encyclopedia of Machine Learning*, C. Sammut and G. Webb, Editors. 2010, Springer US. p. 36-39.

24.   Blum, C. and X. Li, *Swarm intelligence in optimization.* 2008: Springer.

25.   Blum, C., *Ant colony optimization: Introduction and recent trends.* Physics of Life reviews, 2005. **2**(4): p. 353-373.

26.   Elbery, A. and H.A. Rakha, *A Novel Stochastic Linear Programming Feedback Eco-routing Traffic Assignment System.* 2017.

27.   Brzezinski, D.J., Enns, P, and Hart, C., *Facility-specific speed correction factors. MOBILE6 Stakeholder Review Document.* U.S. Environmental Protection Agency (EPA), 1999.

28.   ARB, C.A.R.B., *User's Guide to EMFAC, Calculating emission inventories for vehicles in California.* 2007.

29.   Rakha, H., et al. *Emission model development using in-vehicle on-road emission measurements.* in *Annual Meeting of the Transportation Research Board, Washington, DC.* 2004.

30.   Barth, M., An, F., Younglove, T., Scora, G., Levine, C., Ross, M., and Wenzel, T. , *Comprehensive modal emission model (CMEM) version 2.0 user's guide. Riverside, Calif.* 2000.

31.   Elbery, A., et al. *Eco-Routing Using V2I Communication: System Evaluation.* in *Intelligent Transportation Systems (ITSC), 2015 IEEE 18th International Conference on.* 2015. IEEE.

32.   *Trial-Use Standard for Wireless Access in Vehicular Environments (WAVE) - Resource Manager.* IEEE Std 1609.1-2006, 2006: p. 1-71.

33.   *IEEE Draft Guide for Wireless Access in Vehicular Environments (WAVE) - Architecture.* IEEE P1609.0/D5, September 2012, 2013: p. 1-74.

34.   Jiang, D., et al., *Design of 5.9 GHz DSRC-based vehicular safety communication.* Wireless Communications, IEEE, 2006. **13**(5): p. 36-43.

35.   Hafeez, K.A., et al., *Performance Analysis and Enhancement of the DSRC for VANET's Safety Applications.* Vehicular Technology, IEEE Transactions on, 2013. **62**(7): p. 3069-3083.

36.   Hafeez, K.A., et al. *A New Broadcast Protocol for Vehicular Ad Hoc Networks Safety Applications*. in *Global Telecommunications Conference (GLOBECOM 2010), 2010 IEEE*. 2010.

37.   Hafeez, K.A., et al. *Impact of Mobility on VANETs' Safety Applications*. in *Global Telecommunications Conference (GLOBECOM 2010), 2010 IEEE*. 2010.

38.   Yin, J., et al., *Performance evaluation of safety applications over DSRC vehicular ad hoc networks*, in *Proceedings of the 1st ACM international workshop on Vehicular ad hoc networks*. 2004, ACM: Philadelphia, PA, USA. p. 1-9.

39.   Mitropoulos, G.K., et al., *Wireless Local Danger Warning: Cooperative Foresighted Driving Using Intervehicle Communication.* Intelligent Transportation Systems, IEEE Transactions on, 2010. **11**(3): p. 539-553.

40.   Van den Broek, T.H.A., J. Ploeg, and B.D. Netten. *Advisory and autonomous cooperative driving systems*. in *Consumer Electronics (ICCE), 2011 IEEE International Conference on*. 2011.

41.   Bauza, R., J. Gozalvez, and J. Sanchez-Soriano. *Road traffic congestion detection through cooperative Vehicle-to-Vehicle communications*. in *Local Computer Networks (LCN), 2010 IEEE 35th Conference on*. 2010.

42.   Lakas, A. and M. Cheqfah. *Detection and dissipation of road traffic congestion using vehicular communication*. in *Microwave Symposium (MMS), 2009 Mediterrannean*. 2009.

43.   Roy, S., et al. *Wireless across road: RF based road traffic congestion detection*. in *Communication Systems and Networks (COMSNETS), 2011 Third International Conference on*. 2011.

44.   Drira, W., et al., *ADCS: An Adaptive Data Collection Scheme in Vehicular Networks using 3G/LTE.*

45.   http://www.riverbed.com/products/performance-management-control/opnet.html. Riverbed Technology, Accessed March 2015.